2

Cooperative Systems

This chapter summarizes recent works that relate to the problems studied in this book. Our objective is to make the reader aware of the many considerations involved, highlight the particular scenarios that we study throughout the book, and encourage further work in the area.

2.1 Relaying Protocols

In cooperative diversity, nodes can cooperate with each other to provide spatial diversity gain at the destination. In this case, at any given time, any node can be a source, relay, or destination. The function of the relay node is to assist in the transmission of the source information to the destination node. To ensure diversity gains, this relay is chosen in such a way that its link to the destination is independent from that of the source. Within the framework of cooperative diversity, there are two main cooperative diversity techniques for transmission between a pair of nodes through a multiple relay nodes: AF [21] and DF [15], [12] modes. In the AF mode, the relay terminal simply amplifies and retransmits the signal received from the source terminal (the signal received at the relay terminal is corrupted by fading and additive noise). No demodulation or decoding of the received signal is performed in this case. On the other hand, in the DF mode, the signal received from the source node is demodulated and decoded before retransmission.

Most of the previous research on un-coded cooperative diversity adopts AF protocols [23]-[29]. However, for AF, when the instantaneous channel state information (CSI) is not available to the receivers, satisfying the relay power constraints greatly complicates the demodulation as well as analysis [24]. Obviously, the DF protocols require more processing than AF, as the signals have to be decoded and then re-encoded at the relay transmission. However, if signals

are correctly decoded at relays, performances are better than those of AF protocols, as noise is deleted. In addition, the DF can be extended to combine coding techniques and might be easier to incorporate into network protocols [26]-[29].

Relay channels are central to our study of cooperative diversity. Many of the initial works performed in this area have focused on additive white Gaussian noise (AWGN) channels, and examined the performance in terms of the well-known Shannon capacity [30]. The classical relay channel models a class of three terminal communication channels, originally introduced and examined in [31], [32], and subsequently studied by a number of authors, primarily from the information theory community. In general, the distinctive property of relay channels is that certain terminals, i.e., relay nodes, receive, process, and re-transmit some information bearing signal of interest to a certain destination in order to improve the performance of the system.

Cover and El Gamal [33] examined certain non-faded relay channels, and developed lower and upper bounds on the channel capacity via random coding. Generally these lower and upper bounds do not coincide, except in the class of degraded relay channels [33]. These lower bounds on capacity, i.e., achievable rates, are obtained via three structurally different random coding schemes, referred to in [33] as facilitation, cooperation, and observation.

Many configurations arise for cooperative diversity in wireless settings. In what follows, we denote the source, relay, destination nodes by *S*, *R*, and *D*, respectively. Figure 2.1 depicts a number of these configurations. For example, the classical relay channel in Figure 2.1(a) reduces to direct transmission when the relay is removed, and cascade transmission when the destination cannot receive (or ignores) the source transmission. Figure 2.1(b) represents the parallel relay channel without direct transmission. The configurations in Figure 2.1(c)-(e)

represent a classical multiple-access channel, broadcast channel, and interference channel, respectively.

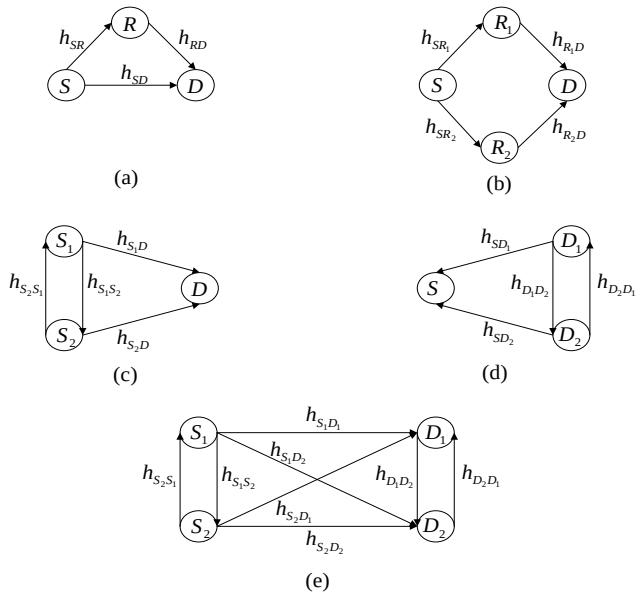

Figure 2.1 *Various relaying configurations that arise in wireless networks: Classical relay channel, (b) parallel relay channel, (c) multiple-access channel with relaying, (d) broadcast channel with relaying, (e) interference channel with relaying.*

Of the remaining configurations depicted in Figure 2.1, only parallel relay channels (see Figure 2.1(b)) and multiple-access channels with relaying (see Figure 2.1(c)) have received attention in the literature. Schein and Gallager [34] introduced the parallel relay channel model in an attempt to make the classical relay channel symmetric.

Most of the work that has been done in the area of cooperative networks considered three main types of TDMA-based transmission protocols. These protocols are termed Protocols I, II and III and they were proposed in [15]-[17], respectively. Protocols I, II and III convert the spatially distributed antenna system into effective MIMO, single-input multiple-output (SIMO) and

multiple-input single-output (MISO), respectively. We should mention that Protocol II has been the most popular due to its simplicity and performance. All of the previous works assume that transmission takes place in a half-duplex fashion (the nodes cannot transmit and receive simultaneously) in all relays over two separate time slots. Since our work will use these transmission protocols, in the following, we shall briefly describe the details of these three protocols in the un-coded DF and AF modes.

2.1.1 System Model

Protocol I. In the AF mode, the source node transmits the signal to both the destination and relay nodes during the first time slot (see Figure 2.2(a)). The signals received at the destination and the relay nodes in the first time slot are given by

$$y_{SD}(t_1) = \sqrt{E_{SD}} h_{SD} s_1 + n_{SD}(t_1), \tag{2.1}$$

$$y_{SR}(t_1) = \sqrt{E_{SR}} h_{SR} s_1 + n_{SR}(t_1), \tag{2.2}$$

where s_1 is the symbol transmitted in the first time slot t_1; E_{SD}, and E_{SR} represent the transmitted signal energy for the corresponding link; h_{SD}, and h_{SR} are the complex fading channel coefficients with unit-power gain; $n_{SD}(t)$, and $n_{SR}(t)$ are AWGN samples with zero mean and variance $N_0/2$ per dimension.

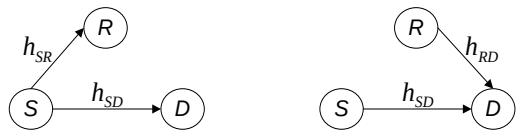

Figure 2.2 *Protocol I: (a) the first time slot, (b) the second time slot.*

In the second time slot, both the relay, and the source nodes transmit the signal

to the destination node (see Figure 2.2 (b)). The signals received at the destination in the second time slot are then given by

$$y_{SD}(t_2) = \sqrt{E_{SD}} h_{SD} s_2 + n_{SD}(t_2), \tag{2.3}$$

$$y_{RD}(t_2) = h_{RD} A_{RD} y_{SR}(t_1) + n_{RD}(t_2),$$

$$= h_{RD} A_{RD} \left(\sqrt{E_{SR}} h_{SR} s_1 + n_{SR}(t_1) \right) + n_{RD}(t_2), \tag{2.4}$$

where s_2 is the symbol transmitted in the second time slot t_2; h_{RD} is the complex fading channel coefficient with unit-power gain; $n_{RD}(t_2)$ is AWGN samples with zero mean and variance $N_0/2$ per dimension; A_{RD} is the amplification factor at the relay node. One choice for the amplification gain was given in [25] to be

$$A_{RD}^2 = \frac{E_{RD}}{E_{SR} |h_{SR}|^2 + \frac{N_0}{2}}, \tag{2.5}$$

where E_{RD} is the transmitted signal energy from the relay node. One can rewrite (2.4) as

$$y_{RD}(t_2) = h_{RD} A_{RD} \sqrt{E_{SR}} h_{SR} s_1 + n_{SRD}, \tag{2.6}$$

where $n_{SRD} = h_{RD} A_{RD} n_{SR}(t_1) + n_{RD}(t_2)$. The signals received at the destination node over two time slots are then given by

$$y_{D_1} = y_{SD}(t_1) = \sqrt{E_{SD}} h_{SD} s_1 + n_{SD}(t_1), \tag{2.7}$$

$$y_{D_2} = y_{SD}(t_2) + y_{RD}(t_2) = \sqrt{E_{SD}} h_{SD} s_2 + n_{SD}(t_2) + h_{RD} A_{RD} y_{SR}(t_1) + n_{RD}(t_2)$$

$$= \sqrt{E_{SD}} h_{SD} s_2 + n_{SD}(t_2) + h_{RD} A_{RD} \left(\sqrt{E_{SR}} h_{SR} s_1 + n_{SR}(t_1) \right) + n_{RD}(t_2)$$

$$= h_{RD} A_{RD} \sqrt{E_{SR}} h_{SR} s_1 + \sqrt{E_{SD}} h_{SD} s_2 + n_D, \tag{2.8}$$

where $n_D = n_{SD}(t_2) + h_{RD} A_{RD} n_{SR}(t_1) + n_{RD}(t_2)$. Protocol I in the AF mode can now be summarized as

$$Y_{P_{I-AF}} = H_{P_{I-AF}} S + N_{P_{I-AF}}, \tag{2.9}$$

where $Y_{P_{I-AF}} = [y_{D_1} \quad y_{D_2}]^T$ is the received signal vector; the superscript $(\cdot)^T$ stands for transpose; $N_{P_{I-AF}} = [n_{SD}(t_1) \quad n_D]^T$ is the noise vector; $S = [s_1 \quad s_2]^T$ is transmitted signal vector; $H_{P_{I-AF}}$ is the complex fading channel matrix given by

$$H_{P_{I-AF}} = \begin{bmatrix} \sqrt{E_{SD}}h_{SD} & 0 \\ h_{RD}A_{RD}\sqrt{E_{SR}}h_{SR} & \sqrt{E_{SD}}h_{SD} \end{bmatrix}. \tag{2.10}$$

In the DF mode, the source node transmits the signals to both the destination and the relay nodes during the first time slot. The signals received at the destination node and the relay nodes in the first time slot are given by (2.1) and (2.2), respectively. Different from the AF mode, in the DF mode, the relay node demodulates and decodes the received signal during the first time slot. Assuming that the signal is decoded correctly and retransmitted, we obtain

$$y_{RD}(t_2) = \sqrt{E_{RD}}h_{RD}s_1 + n_{RD}(t_2). \tag{2.11}$$

Similar to the AF mode, Protocol I in the DF mode can now be summarized as

$$Y_{P_{I-DF}} = H_{P_{I-DF}}S + N_{P_{I-DF}}, \tag{2.12}$$

where $Y_{P_{I-DF}} = [y_{D_1} \quad y_{D_2}]^T$ is the received signal vector;
$N_{P_{I-DF}} = [n_{SD}(t_1) \quad (n_{SD}(t_2) + n_{RD}(t_2))]^T$ is the noise vector; $S = [s_1 \quad s_2]^T$ is transmitted signal vector; $H_{P_{I-DF}}$ is the complex fading channel matrix given by

$$H_{P_{I-DF}} = \begin{bmatrix} \sqrt{E_{SD}}h_{SD} & 0 \\ \sqrt{E_{RD}}h_{RD} & \sqrt{E_{SD}}h_{SD} \end{bmatrix}. \tag{2.13}$$

The spectral efficiency of Protocol I is given by

$$\mathrm{H} = \frac{R_b}{B} = \frac{R_s k \log_2 M}{R_s p} = \frac{k \log_2 M}{p} = \frac{2 \log_2 M}{2} = \log_2 M \ \text{ bits/s/Hz} \tag{2.14}$$

where k is the number of symbols of the source node, p is the number of

transmission periods to transmit symbols, R_b is the bit rate, R_s is the symbol rate, M is the constellation size, and B is the bandwidth.

Protocol II. In this protocol, in the first time slot, the source node sends a message to both the relay and the destination nodes (see Figure 2.3(a)). In the second time slot, the relay node sends to the destination node (see Figure 2.3(b)).

In the AF mode, the received signal at the destination node for Protocol II can be written as

$$Y_{P_{II-AF}} = H_{P_{II-AF}} s_1 + N_{P_{II-AF}}, \tag{2.15}$$

where $Y_{P_{II-AF}} = [y_{D_1} \quad y_{D_2}]^T$ is the received signal vector; $N_{P_{II-AF}} = [n_{SD}(t_1) \quad (n_D - n_{SD}(t_2))]^T$ is the effective noise vector; s_1 is transmitted signal; $H_{P_{II-AF}}$ is the first column of $H_{P_{I-AF}}$ in (2.10).

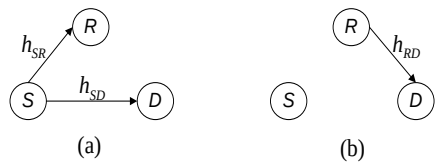

Figure 2.3 *Protocol II: (a) the first time slot, (b) the second time slot.*

In the DF mode, the received signal at the destination node for Protocol II can be rewritten from (2.12) as

$$Y_{P_{II-DF}} = H_{P_{II-DF}} s_1 + N_{P_{II-DF}}, \tag{2.16}$$

where $Y_{P_{II-DF}} = [y_{D_1} \quad y_{D_2}]^T$ is the received signal vector; $N_{P_{II-DF}} = [n_{SD}(t_1) \quad n_{RD}(t_2)]^T$ is the effective noise vector; $H_{P_{II-DF}}$ is the first column of $H_{P_{I-DF}}$ in (2.13).

The spectral efficiency of Protocol I is given by

$$\mathrm{H} = \frac{R_b}{B} = \frac{R_s k \log_2 M}{R_s p} = \frac{k \log_2 M}{p} = \frac{\log_2 M}{2} \text{ bits/s/Hz} \tag{2.17}$$

Protocol III. The source node in this protocol sends a message to the relay node in the first time slot (see Figure 2.4(a)). Both the source and the relay nodes send to the destination node in the second time slot (see Figure 2.4(b)).

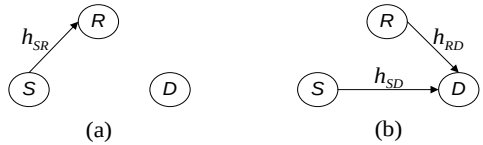

Figure 2.4 *Protocol III: (a) the first time slot, (b) the second time slot.*

In the AF mode, the received signal at the destination node for Protocol III can be written as

$$y_{P_{III-AF}} = H_{P_{III-AF}} S + n_{P_{III-AF}}, \tag{2.18}$$

Where $y_{P_{III-AF}}$ is the received signal; $n_{P_{III-AF}} = n_D$ is the effective noise; $S = [s_1 \quad s_2]^T$ is transmitted signal vector; $H_{P_{III-AF}}$ is the second row of $H_{P_{I-AF}}$ in (2.10).

In the DF mode, the received signal at the destination node for Protocol III can be rewritten from (2.12) as

$$y_{P_{III-DF}} = H_{P_{III-DF}} S + n_{P_{III-DF}}, \tag{2.19}$$

where $y_{P_{III-DF}}$ is the received signal; $n_{P_{III-DF}} = n_{SD}(t_2) + n_{RD}(t_2)$ is the effective noise; $S = [s_1 \quad s_2]^T$ is transmitted signal vector; $H_{P_{III-DF}}$ is the second row of $H_{P_{I-DF}}$ in (2.13).

The spectral efficiency of Protocol III is given by

$$\mathrm{H} = \frac{R_b}{B} = \frac{R_s k \log_2 M}{R_s p} = \frac{k \log_2 M}{p} = \frac{2 \log_2 M}{2} = \log_2 M \text{ bits/s/Hz} \tag{2.20}$$

2.1.2 Simulation Results

Here, we present simulation results for Protocols I, II, and III using BPSK transmission. In all scenarios we assume that there is one relay node. In all of these results, the transmission links (source to relay, source to destination, and relay to destination) are modeled as a quasi-static flat fading channels where the fading coefficients are fixed within a frame and change independently from one frame to another, the receiver has perfect knowledge of the channel coefficients, and the transmitted frame size is equal to 130 symbols. Also we consider equal transmitted energies for the different links, i.e., $E_{SD}=E_{SR}=E_{RD}=E_b$.

Figure 2.5 shows the BER comparisons for Protocols I, II, and III, all operating in the DF mode with error-free recovery at the relay. This assumption, however, seems to be too optimistic and can only be justified under special conditions (i.e., large SNR or un-faded channel between the source and relay). For Figure 2.5, we can see that at the BER of 5×10^{-4}, Protocol II is better by about 11 dB and 14 dB than Protocol I and III, respectively. Also we note that Protocol II achieves full diversity, which is two in this case, while Protocols I and III do not achieve full diversity.

Figure 2.6 shows BER comparisons for Protocols I, II, and III, all operating in the DF mode, considering the effect of channel errors at the relay. From this figure, it can be observed that at the BER of 5×10^{-4}, Protocol II gains about 2 dB and 5 dB relative to Protocol I and III, respectively. Also we note that Protocols I, II, and III do not achieve full diversity.

In Figure 2.7 we perform BER comparisons for Protocols I, II, and III, all operating in the AF mode. From this figure, Protocol II at the BER of 5×10^{-4} is superior by about 9 dB and 14 dB to Protocols I and III, respectively. Also, we

note that Protocol II achieves full diversity, which is two in this case, while Protocols I and III do not achieve full diversity.

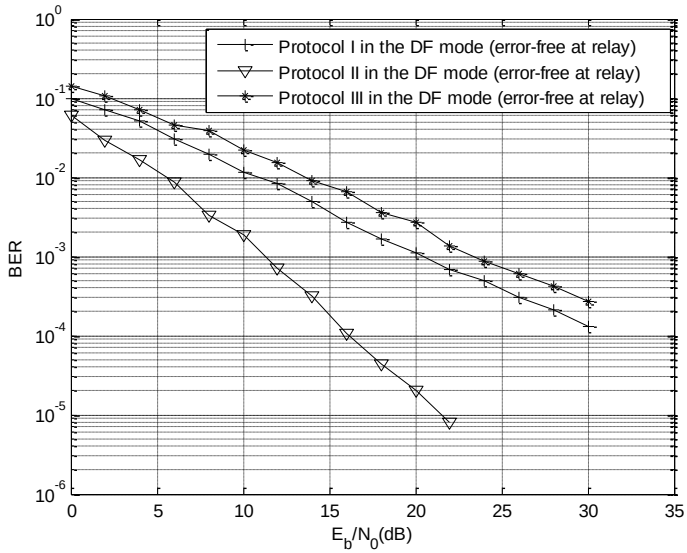

Figure 2.5 *BER comparisons for Protocols I, II, and III in the DF mode (error-free at relay).*

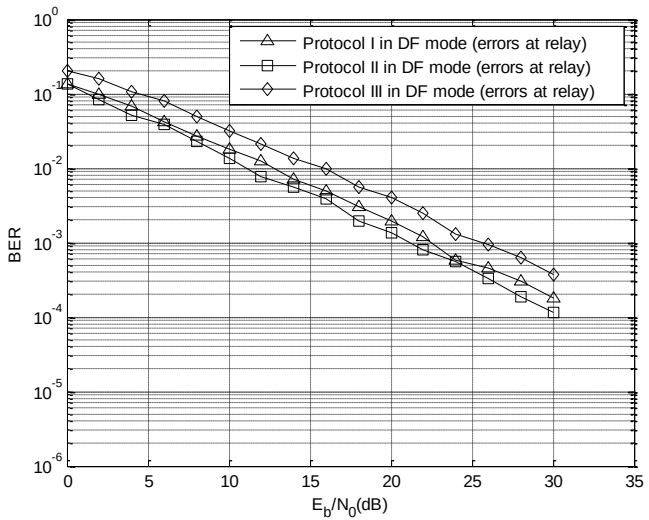

Figure 2.6 *BER comparisons for Protocols I, II, and III in the DF mode (errors at relay).*

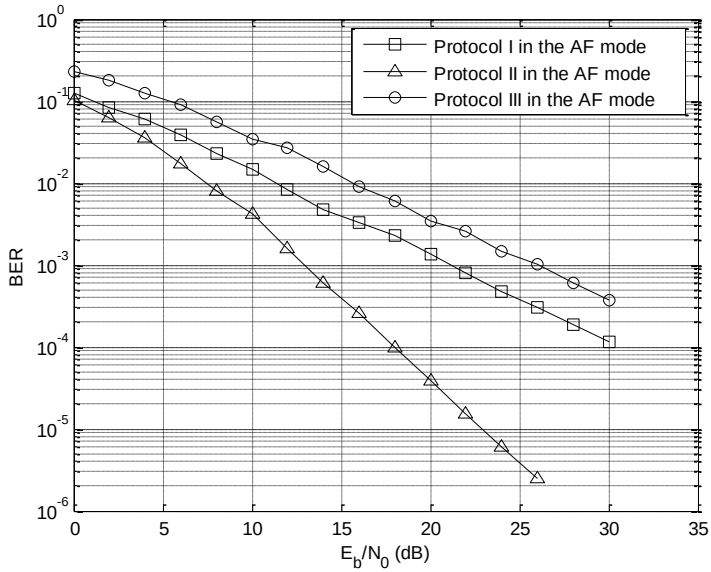

Figure 2.7 *BER comparisons for Protocols I, II, and III in the AF mode.*

2.2 Coded Cooperation

In the previous section, we have seen that the performance of un-coded multi-relay systems when the nodes operate in the DF mode degrades. This was shown via simulations. Based on the results we have obtained so far, it is clear that the diversity of multi-relay systems is very sensitive to the decoded errors at the relays. This suggests that improving the reliability of detection at the relays should improve the diversity.

Coded cooperative communication has been a very active research topic in recent years. In [13], [14], Sendonaris et al. demonstrated that cooperation among users not only leads to higher data rates, but also to decrease sensitivity to channel variations. They have also shown that spatial diversity can be obtained using the partnering user, even if the inter-user channel is noisy. Laneman et al. [16] developed several cooperative protocols which can achieve full diversity.

The goal was to minimize the outage probability. Recently, channel coding for cooperative systems has been studied in [35]-[37].

For instance, Hunter and Nosratinia [35] used rate-compatible punctured convolutional (RCPC) codes for the partnering users and cyclic redundancy check (CRC) at the partner to arrive at an efficient coding scheme for cooperation. Along the same lines, Stefanov and Erkip [37] provided a frame-error rate (FER) analysis to show that coded cooperation can achieve full diversity. They illustrated that when different users experience independent fades, the block-fading channel model is appropriate for coded cooperation, and the framework in [38] can be used for code design. Liu et al. [36] considered punctured turbo codes for cooperation with a strict decoding delay constraint, and analyzed the FER behavior. Some recent work includes cooperative STC, where the partnering nodes may have multiple antennas [39].

In [22], the authors considered space-time coded cooperation schemes for multi- relay channels. The first scheme is a repetition-based cooperative diversity scheme where the destination receives separate signals from each of the relays during the second phase on orthogonal sub-channels. The second one is a space-time-coded cooperative diversity scheme, in which relays utilize a suitable space-time code in the second phase and therefore can transmit simultaneously on the same sub-channel.

In [35], [37], [39]-[41], the authors proposed cooperative diversity with classical DF. The key idea is that each user transmits its own bits in the first frame. Each user also receives and decodes the partner's transmission. If the user successfully decodes the partner's code word, determined by checking the CRC bits, the user computes and transmits additional parity bits for the partner's data in the second frame. In [42], [43], the authors considered cooperative diversity with superposition modulation. In the superposition modulated cooperative

transmission system, a node transmits its own signal superimposed on other node's signal to the destination node.

The schemes that we consider most related to our work are the ones proposed in [35], [37], [39]-[41]. In light of this, coded cooperation in essence splits each code- word into two partitions, each of them is transmitted in a distributed manner to ensure large coding gains relative to conventional coding schemes (i.e., non-cooperative systems). In addition to the coding advantage, coded cooperation is based on incremental redundancy and thus allows a more flexible bandwidth allocation between the source and relay nodes, as compared to repetition coding.

In the following, we shall briefly describe the details of Schemes I, II that are related to our work. Scheme I is the one proposed in [35], [40], [41] and Scheme II is the one proposed in [37], [39].

2.2.1 System Model

Scheme I. In this scheme, the users segment their source data into blocks which are augmented with a CRC code, for a total of *K* bits per source block (including the CRC bits). Each block is then encoded with a forward error-correcting code, so that, for an overall rate *R* code, we have $N = K/R$ total code bits per block. Figure 2.8 illustrates the general coded cooperation frame work.

The two users cooperate by dividing the transmission of their *N*-bit code words into two successive time segments, or frames. In the first frame, each user transmits a rate $R_1 > R$ code word with $N_1 = K/R_1$ bits. This it is a valid (albeit weaker) code word which can be decoded to obtain the original information. Each user also receives and decodes the partner's transmission. If the user successfully decodes the partner's rate R_1 code word, determined by

checking the CRC bits, the user computes and transmits N_2 additional parity bits for the partner's data in the second frame, where $N_1 + N_2 = N$. These additional parity bits are selected such that they can be combined with the first frame code word to produce a more powerful rate R code word. If the user does not successfully decode the partner, N_2 additional parity bits for the user's own data are transmitted. Each user always transmits a total of N bits per source block over the two frames, and the users only transmit in their own multiple access channels.

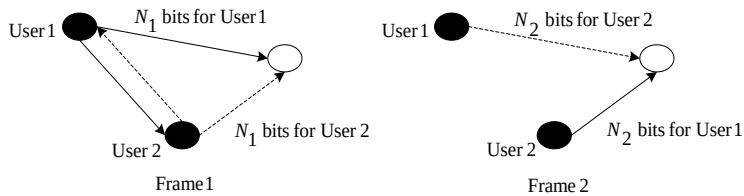

Figure 2.8 *Cooperative transmission scheme.*

In general, various channel coding methods can be used within this coded cooperation framework. For example, the overall code may be a block or convolutional code, or a combination of both. The code bits for the two frames may be partitioned through puncturing, product codes, or other forms of concatenation. In this scheme, the overall rate R code is selected from a given RCPC code family (e.g., the mother code). The code word for the first frame is obtained by applying the puncturing matrix corresponding to rate R_1, and the additional parity bits transmitted in the second frame are those punctured from the first frame. Figure 2.9 illustrates a user's implementation of coded cooperation using RCPC codes.

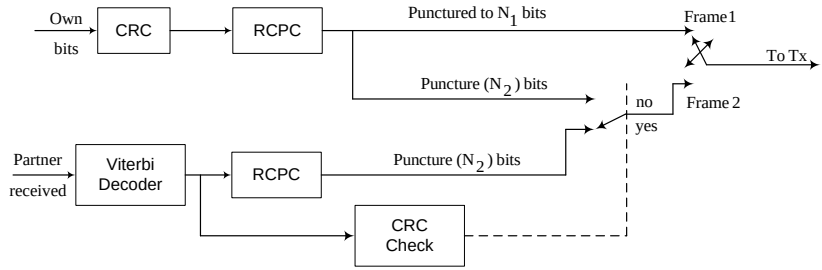

Figure 2.9 *A user's implementation of coded cooperation with RCPC codes.*

The users transmit on orthogonal channels (e.g., TDMA, code-division multiple- access (CDMA), or frequency-division multiple-access (FDMA)), which allows the destination, and other users in the cooperative case, to separately detect each user. In scheme I, BPSK modulation is assumed, for which the baseband-equivalent discrete- time signal transmitted by user $i \in \{1,2\}$ and received by user $j \in \{0,1,2\}$ ($j \neq i$, and $j = 0$ denotes the destination) is given by

$$r_{ij}(t) = h_{ij}(t)\sqrt{E_{ij}}\,x_i(t) + n_j(t), \tag{2.21}$$

where E_{ij} is the transmitted energy per bit for user i, $x_i(t) \in \{-1,+1\}$ is the BPSK modulated code bit at time t, $h_{ij}(t)$ is modeled as complex Gaussian distributed with zero mean and unit variance, representing the fading channels between users i and j, and $n_j(t)$ accounts for noise and other additive interference at the receiver. For slow (quasi-static) fading, the fading coefficients remain constant ($h_{ij}(t) = h_{ij}$) over the transmission of each source frame. The noise term $n_j(t)$ is modeled as independent, zero-mean AWGN with variance $N_0/2$ per dimension.

The instantaneous received SNR for the channel between users i and j is defined as

$$\gamma_{i,j}(t) = \frac{|h_{i,j}(t)|^2 E_{i,j}}{N_0} \tag{2.22}$$

For $|h_{i,j}(t)|$ Rayleigh distributed, $\gamma_{i,j}(t)$ has an exponential distribution with mean

$$\bar{\gamma}_{i,j} = E[\gamma_{i,j}(t)] = E\left[\frac{|h_{i,j}(t)|^2 E_{i,j}}{N_0}\right] = \frac{E_{i,j}}{N_0} E\left[|h_{i,j}(t)|^2\right] \tag{2.23}$$

where $E[\cdot]$ denotes the expectation operator; $|h_{i,j}|^2$ is constant over t for a given channel.

Scheme II. In this scheme, the cooperative system is shown in Figure 2.10. For each node, the information bits are encoded by a channel encoder. The coded symbols are properly multiplexed for cooperation. The multiplexed symbols are passed through a serial-to-parallel converter, and are mapped to a particular signal constellation. When node S_i, transmits, the output of the modulator at each discrete time slot t is the signal $x_i(t)$.

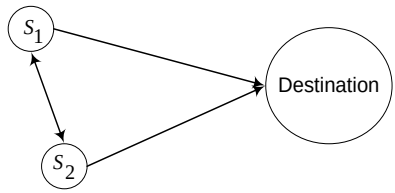

Figure 2.10 *Cooperative system.*

The received signal at the destination at time t due to transmission from S_i is given by

$$y_{i,j}(t) = h_{i,j}(t)\sqrt{E_{i,j}}\,x_i(t) + z_j(t), \tag{2.24}$$

where the noise samples, zj (t), are modeled as independent realizations of a zero-mean complex Gaussian random variable with variance $N_0/2$ per dimension.

Using time division, each user has a separate time slot consisting of coded symbols (see Figure 2.11(a)). For the cooperative scheme, each user divides its own time slot into two equal segments, as shown in Figure 2.11(b). Along with channel coding for error correction, the users also perform a CRC for error detection. To optimize the performance of coded cooperative system, S_1 can transmit any portion of coded bits. For simplicity, S_1 uses the first segment of its time slot to transmit half of its coded symbols. These symbols are obtained by multiplexing the original coded symbol stream. Both the destination and the partner receive these coded symbols. Note that for the rate $1/4$ convolutional code, the effective code rate that the partner observes is $1/2$. If S_2 can successfully decode (as indicated by the CRC), it re-encodes the information bits to get the additional coded symbols which were not originally transmitted by S_1. These coded symbols are transmitted by S_2 for S_1 in the second segment of S_1's time slot. Hence, the destination observes half of the coded symbols through the S_1 destination link, the remaining half through the S_2 destination link.

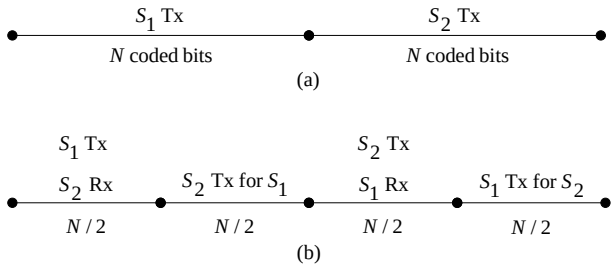

Figure 2.11 *Time-division channel allocations. (a) Orthogonal direct transmission. (b) Orthogonal cooperative diversity transmission.*

These links were assumed to have independent quasi-static fading, leading to an overall block-fading channel from the perspective of the destination. This provides additional diversity, obtained through the partner's link toward the destination.

If S_2 cannot receive the source's information correctly, using one bit of information, it notifies S_1 that there was a failure in decoding, and S_1 continues transmission. As far as the destination is concerned, it does not matter whether the second segment of coded bits comes from S_1 or its partner. It is assumed that the destination estimates the channel attenuation every N/2 symbols, hence, the decoding algorithm remains unchanged. Note that by coded cooperation, S_1 does not decrease its information rate. Finally, S_1 and S_2 change roles for the time slot of S_2. Since the inter-user channel from S_1 to S_2 has the same average quality with S_2 to S_1 channel, with cooperation, both nodes continue to meet their individual average power constraints.

2.2.2 Simulation Results

Here, we present our simulation results for Schemes I, II that are related to our work. In all of these results, we assume that the cooperative node operates in the DF mode. For simplicity, BPSK modulation is assumed. The different sub-channels between the source, relay, and destination are assumed to be independent flat Rayleigh fading channels. Also, we consider a quasi-static fading channel where the channel coefficients are fixed for the duration of the frame and change independently from one frame to another. In all simulations, the transmitted frame size is equal to 130 coded bits, and equal transmitted energies in both schemes for the different links is considered, i.e., $\gamma_{1,0} = \gamma_{2,0} = E_b/N_0$ but from user to destination node, $\gamma_{1,2} = \gamma_{2,1}$, can be different.

The convolutional code used is of constraint length four and generator polynomials $(13, 15, 15, 17)_{\text{octal}}$ [44]. When the relay cooperates with the source node, the source transmits the code words corresponding to rate 1/2, $(13, 15)_{\text{octal}}$

convolutional code to the relay and destination nodes in the first frame. The relay node receives this codeword and decoding is performed to obtain an estimate of the source information bits. In the second frame, both the relay and source nodes transmit the code words corresponding to rate 1/2, $(15, 17)_{\text{octal}}$ convolutional code to the destination node.

Figure 2.12 shows a comparison of the BER performance of Schemes I and II for one relay channel operating in the DF mode when the effect of channel errors at relay is considered (i.e., $\bar{\gamma}_{1,2} = \bar{\gamma}_{2,1} = 8\,dB$). We also include in the same figure the performance of these schemes with perfect detection at the relay. To maintain the same average power, the source and relay nodes divide their power according to the ratio 1/2. As shown from these results, the performance of Scheme II is 0.5 dB better than Scheme I. The 0.5-dB penalty incurred is due to the use of RCPC code. Also, the diversity gain achieved using one relay is evident from these results.

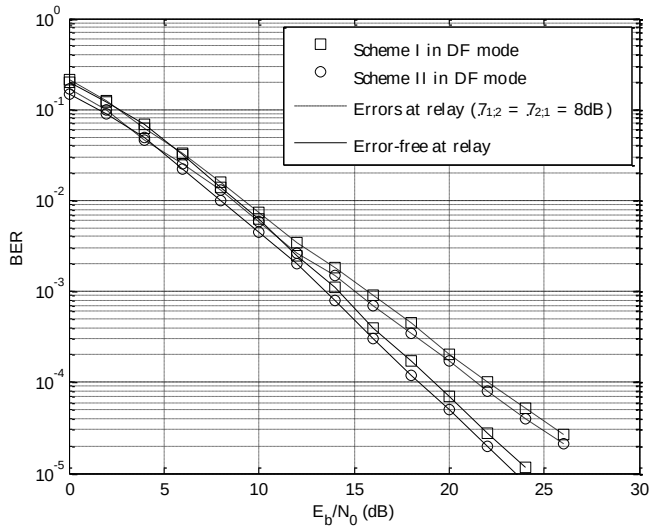

Figure 2.12 *BER comparisons for Schemes I, II in the DF mode with error-free detection at relay node, and* $\bar{\gamma}_{1,2} = \bar{\gamma}_{2,1} = 8\,dB$ *with relay errors.*

2.3 Antenna/Relay Selection

Antenna selection has been considered before for centralized MIMO systems where it was shown that impressive diversity and coding gains can be achieved [45]-[49]. The idea behind antenna selection is to use only a subset of the available antennas. The consequence of this is that, while taking advantage of the benefits of the available antennas, the number of RF chains is reduced to the number of selected antennas, which results in complexity reduction. A natural extension of antenna selection is relay selection, whereby the relay that enjoys the best reliability is selected. To accomplish this, the source will have to know the reliability of the available nodes through some feedback to decide on what relay to use for relaying. It is also possible to select multiple relays for cooperation.

In [45], the authors studied the impact of antenna selection at the receiver on the diversity order and coding gain provided by the underlying STC. It was shown that, for full-rank STTC codes and quasi-static fading channels, the diversity order of the underlying STTC code is maintained. A comprehensive performance analysis of STBCs with receive antenna selection was presented in [46]. They showed that the diversity order with antenna selection is maintained as that of the full complexity system. The performance of a serial concatenated scheme comprising a convolutional code and a STBC separated by an inter leaver was studied in [47]. They showed that the use of antenna selection at the receiver side only affects the SNR coding gain, but not the overall diversity order. This phenomena was evident for both the fast and block flat fading channel models.

In [48], algorithms for exact channel knowledge and statistical channel knowledge selection with the antenna sets selected to minimize the probability of error were presented. They showed that when exact channel knowledge is available, the selection algorithm chooses the antenna subsets that minimizes the

instantaneous probability of error and maximizes the SNR. The combination of transmit antenna selection with STBC scheme was considered in [49]. They showed that if all the transmit antenna were used, then this scheme achieves a full diversity order with simple decoding complexity.

In Chapter 4, we consider antenna/relay selection for coded cooperative networks in an effort to improve their end-to-end performance by improving the detection reliability at the relay nodes. Considering DF and AF relaying, we analyze the impact of antenna/relay selection on the performance of cooperative networks in conjunction with the distributed coding scheme introduced in Chapter 3. Specifically, we derive upper bounded expressions for the bit error rate assuming M -PSK transmission. Our analytical results show that the maximum diversity order of the system is maintained for the entire range of BER of interest, unlike the case without antenna/relay selection. Several numerical and simulation results are presented to demonstrate the efficacy of the proposed scheme.

2.4 Channel Estimation

Coherent reception requires the receiver to acquire channel knowledge to compensate for the channel induced distortions. The process of acquiring the channel knowledge is called channel estimation and is an integral part of most communication systems. Apart from the knowledge of channel statistics, the channel estimator also requires knowledge of the instantaneous channel values to track the channel fading and compensate it. Typically, known symbols called “pilot” symbols are multiplexed along with the data to aid the receiver in channel estimation [50]-[58].

STC modulation with multiple transmits and/or multiple receive antennas and orthogonal pilot sequence insertion was proposed in [50]. In this scheme, the

transmitter inserts periodic orthogonal pilot sequences in each one of the simultaneously transmitted blocks. Each block is then pulse-shaped and transmitted from a different antenna. Since the signal at each receive antenna is a linear superposition of the transmitted signals, the receiver uses orthogonal pilot sequences to estimate the different fading channels. The receiver then uses an appropriately designed interpolation filter to interpolate those estimates and obtain accurate CSI. The problem of training sequence design for multiple-antenna transmissions over quasi-static frequency-selective channels was addressed in [51]. In [51] various methods to identify good training sequences for systems employing multiple transmit antennas over frequency-selective channels were studied.

In [52], multiple-antenna wireless communication links with training-based schemes were addressed. They showed that if optimization over the training and data powers is allowed, then the optimal number of training symbols is always equal to the number of transmit antennas. They also showed that if the training and data powers are instead required to be equal, then the optimal number of symbols can be larger than the number of antennas. In [53], the authors proposed linear dispersion space-time codes in wireless relay networks. It was shown that the source and relay nodes do not have any channel information but the destination has knowledge of both the source to relay channel and relay to the destination channel.

In [54], it is assumed that the relays do not have any channel information, while the destination has only a partial-channel knowledge, by which mean that destination knows only the relay-to-destination channel. In [55], the authors considered pilot symbol aided channel estimation for AF relay based cooperation diversity systems. They investigated the impact of the underlying channel on the pilot insertion strategy and estimator design. In [56], a proposed coherent distributed space-time coding in AF relay networks using training and channel estimation scheme was proposed. It was shown that the relay nodes do not

perform any channel estimation using the training symbols transmitted by the source but instead simply amplify and forward the received training symbols.

The training based channel estimation for AF based relay networks was proposed in [57]. The overall channel from source to destination is estimated at the destination only while the relays amplify and retransmit the information to the destination. In [57], both the least square (LS) and the minimum mean square error (MMSE) channel estimation approaches were considered. In [58], a differential transmission scheme for wireless relay networks using the ideas of distributed space-time coding and differential space-time coding was proposed. The authors showed that compared to coherent distributed space-time coding, distributed differential space-time coding performs 3 dB worse.

In the above works [53]-[57], it has been shown that the source and relay nodes do not have any channel information but the destination has a full/partial channel knowledge. Also the proposed schemes assumed AF relaying but not DF relaying. To this end, we will show in Chapter 5 that the source, relay, and destination nodes do not have any channel information. So in Chapter 5 we propose to use the same coding scheme introduced in Chapter 3 with an imperfect channel estimation and distributed space-time coding cooperation using Alamouti scheme.